Finding the wedge-shaped Au nanoclusters at the surface of GaAs and investigating them with the polarization spectroscopy of plasmons

© V.L. Berkovits[1], V.A. Kosobukin[1], V.P. Ulin[1], P.A. Alekseev[1], F.Yu. Soldatenkov[1], A.V. Nashchekin[1], S.A. Khakhulin[2], O.S. Komkov[2]

[1] Ioffe Institute,
194021 St. Petersburg, Russia
[2] St. Petersburg State Electrotechnical University „LETI",
197376 St. Petersburg, Russia
E-mail: vladimir.berkovits@mail.ioffe.ru

Received May 18, 2023
Revised August 21, 2023
Accepted August 25, 2023

Using high-temperature annealing of thin gold nanofilms deposited onto the (001) surface of doped *p*-GaAs crystal with an ultrathin oxide layer, the nanoclusters of gold (Au_2Ga alloy) are fabricated. The gold clusters have the wedge shapes with rectangular bases elongated in [110] direction at GaAs(001) surface. This assertion is confirmed by the data of diagnostics of Au/*p*-GaAs(001) structures. Anisotropic plasmons localized on equally oriented wedge-shaped Au (Au_2Ga) clusters are investigated with the optical reflectance anisotropy spectroscopy and spectroscopy of polarized light reflection. It is shown that the spectral peak at the energy about 0.9 eV in the near infrared range is associated with plasmons polarized along the longest sides of clusters in crystallographic direction [110]. Another peak — at the energy of 1.8 eV — is due to plasmons having polarization in direction [1$\bar{1}$0].

Keywords: Au-GaAs interaction, wedge-shaped Au clusters, anisotropic plasmons, polarization spectroscopy.

1. Introduction

Combination of optical properties of a semiconductor and plasmons localized on metal nanoclusters is of particular importance for nanophotonics and its applications [1]. This makes it relevant to develop technologies for creation and research of plasmonic metal-semiconductor nanostructures with unusual optical properties. In this direction, methods for preparation of chemically pure gold nanoclusters on GaAs surfaces were developed for Au/GaAs pair traditional in electronics [2,3]. Used for this purpose was high-temperature annealing of Au films deposited on GaAs crystal surface. It has been established in [2–4] that the features of formed Au clusters (size, shape anisotropy, orientation in the array) depend significantly on the state of surface of GaAs(001) substrate.

This paper discusses the following issues: 1) creating the gold nanoclusters of a new type by annealing Au thin films on the surface of *p*-type GaAs; 2) diagnostics of Au clusters; 3) spectroscopic study of their plasmons. The features of these clusters are 1) crystallographically deterministic elongated wedge shape, 2) strict orientation in [110] direction of GaAs crystal and 3) the presence of plasmon resonances in the near infrared region. Using atomic force microscopy (AFM) and scanning electron microscopy (SEM) it has been found that on annealing the structures at temperature 350°C the metal Au-based clusters are formed directly at the surface of GaAs crystal. The clusters have the shape of wedges with the rectangular bases lying on GaAs(001) surface and the long sides parallel to [110] direction. It has been found by optical spectroscopy methods that the gold nanoclusters possess localized plasmons that exhibit strong polarization anisotropy in [110] and [1$\bar{1}$0] axes on GaAs(001) surface. The energies of plasmons polarized along [110] direction of clusters elongation appear in the infrared region.

2. Creation of nanoclusters and their diagnostics

The structures under study were prepared on oxidized surfaces of *p*-GaAs(001) substrates doped with zinc up to concentration $N_a \sim 10^{18}\,\mathrm{cm}^{-3}$ of acceptors, in which case GaAs surface is covered with an ultrathin layer of oxide [5]. Before depositing gold, the surfaces of substrates were treated in aqueous solution of ammonia (NH_4OH) and washed with deionized water. Gold films with thickness 5–20 nm were deposited on the surfaces of substrates by thermal evaporation in vacuum of 10^{-7} Torr. The obtained Au/*p*-GaAs structures were annealed at temperature 350°C during 30 min.

Characterizing the surfaces of Au/*p*-GaAs structures after annealing was carried out using Ntegra Aura atomic force microscope made by NT-MDT and JSM7001F scanning electron microscope (JEOL, Japan). The results are presented in Figure 1.

Primary AFM characterization of Au/*p*-GaAs structures revealed that before annealing the surface of Au film is even. After annealing, patches elongated in [110] direction were seen in AFM and SEM images of Au film surface. In AFM image presented in Figure 1, *a*, such the patches have the lengths 50–150 nm in [110] direction and the transverse

sizes 20–30 nm; the patches being due to the presence of pits on Au film surface. Profile of the pits formed on annealing is seen from Figure 1, *b*, which presents the cross-section of Au film by (110) plane, shown by dashed line in Figure 1, *a*.

Gold film can interact with GaAs crystal at the places of their direct contact [2,4]. This process is realized because at temperature higher than 250°C the reaction between Au and GaAs occurs in accordance with the scheme [6]

$$\mathrm{Au} + \mathrm{GaAs} \rightarrow \mathrm{Au\text{-}Ga} + (1/4)\mathrm{As}_{4\uparrow}. \qquad (1)$$

The initial stage is removal of arsenic atoms from crystal lattice at temperatures significantly lowered owing to the catalytic action of gold. Then, gold atoms can form an Au-Ga alloy on the crystal surface with released gallium atoms. As demonstrated in [7], at annealing temperature ~ 320°C the elongated pyramidal pits are observed on GaAs surface which are associated with clusters having Au_2Ga composition mainly.

In this regard, it is worth commenting on application of notation Au (Au_2Ga) for obtained clusters in which gold is the initializing and basic element. This notation designates gold nanoclusters including intermetallides with Au-Ga bonds. In accordance with the data of [7] in conditions of our technology the intermetallic Au_2Ga compound should appear most probably in clusters penetrating into GaAs. In plasmon spectroscopy, it is impossible to distinguish between Au and Au_2Ga components entering the clusters, since Au and Ga have dielectric permittivities close to each other. However, optical polarization spectroscopy detects reliably the plasmonic spectral and polarization properties originating in the shape and orientation of Au (Au_2Ga) nanoclusters.

The presence of nanoclusters and their shape are established using SEM images, whose example is presented in Figure 1, *c*. This figure displays Au/*p*-GaAs structure cleavage along (110) plane, perpendicular to [110] direction of elongation of formed Au clusters. The upper part of Figure 1, *c* demonstrates horizontal GaAs(001) surface with a residual Au film, and the lower part shows the cross-section (cleavage) of the structure by vertical (110) plane. From Figure 1, *c*, the triangular cross sections of nanoclusters are seen at GaAs crystal surface elongated in [110] direction perpendicular to the cleavage plane.

We have found that after complete chemical removal of gold from the Au/*p*-GaAs sample, the multiple pits remain from Au (Au_2Ga) nanoclusters on GaAs(001) surface. The pits have the shapes of on-surface rectangles whose long sides ($b = 40$–150 nm) are oriented in [110] direction and the length of short sides is $a \leq 40$ nm. When characterized by AFM method, the triangular cross-sections of these pits are observed in (110) cleavage plane. Their depths $h = 30$–35 nm are estimated from AFM ($1\bar{1}0$) profiles of pits in accordance with the cross-sections of clusters seen in SEM images (Figure 1, *c*).

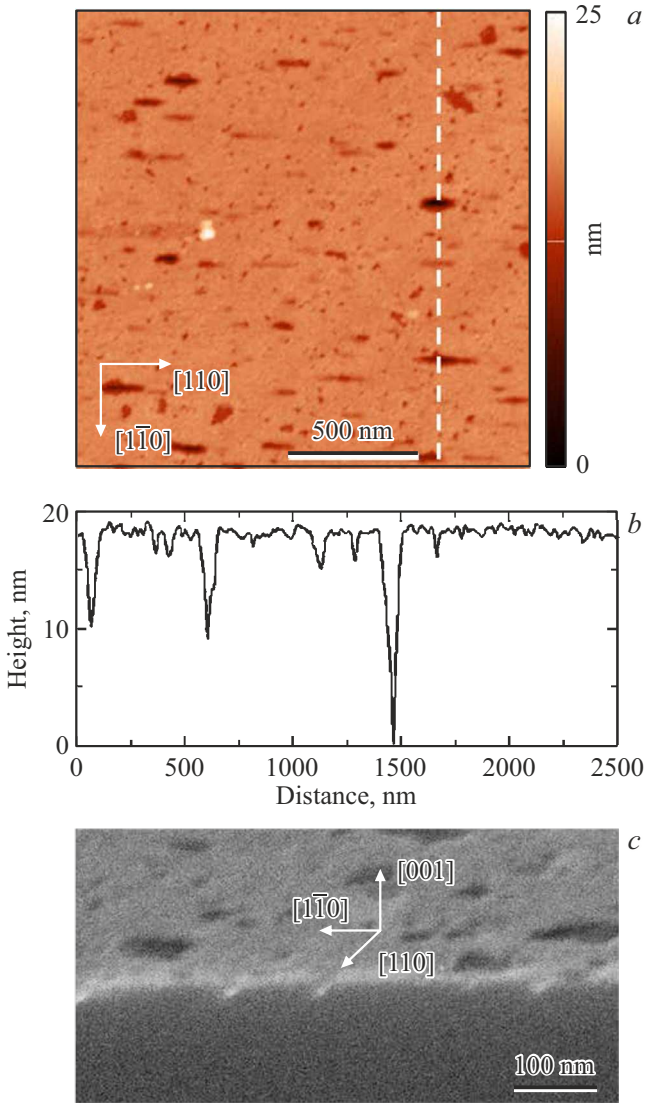

Figure 1. *a* — AFM image of ($2.5 \times 2.5\,\mu$m) fragment of the surface of Au/*p*-GaAs(001) structure after annealing at temperature 350°C during 30 min. *b* — AFM (110) profile of Au film cross-section along the dashed line shown in Figure 1, *a*. *c* — SEM image of Au/*p*-GaAs(001) structure with (110) cleavage plane and Au nanoclusters elongated in [110] direction.

Taking into account the above diagnostics and the results of studying the wedge-shaped clusters Au (Au_2Ga) in GaAs [7], we come to the crystallographic model of nanoclusters depicted in Figure 2, *a*. In agreement with Figure 1, *c* and the data of [7], Au (Au_2Ga) clusters have the shape of wedges with triangular cross-sections and the rectangular bases elongated in [110] direction on GaAs($00\bar{1}$) surface. The end faces of the wedges are formed by ($11\bar{1}$) and ($\bar{1}1\bar{1}$) planes in which Ga atoms are closely packed, and faces ($\bar{1}11$) and ($1\bar{1}1$) similarly occupied by As atoms. This model of a cluster is confirmed by the value 55° obtained from AFM for the dihedral angle between the lateral faces of cluster pits, remaining on GaAs (110) cleavage plane

after removal of Au. Consequently, the wedge-shaped Au (Au_2Ga) nanoclusters and their orientation in GaAs crystal are determined crystallographically. Elongation of such a cluster in [110] direction can be attributed to large rate of Au cluster growth in [110] direction which passes through the end faces with closely packed Ga atoms providing reaction (1).

3. Polarization optical spectroscopy of plasmons

3.1. Experiment

Spectroscopic studies of plasmons localized in gold nanoclusters were carried out to by analogy with [2,3] in the optical scheme sketched in Figure 2, *b*. The presence of plasmon anisotropy in Au/GaAs structures is unambiguously established by reflectance anisotropy spectroscopy. This method measures dependence of the anisotropy signal

$$\frac{\Delta R}{R} = 2\frac{R_x - R_y}{R_x + R_y} \qquad (2)$$

on the frequency ω at normal incidence of light. Here, R_α stands for the coefficient of normal reflection of light polarized along the axis α (x or y) lying in GaAs(001) surface.

In the experiment, the method of reflectance anisotropy spectroscopy is used first to provide a rapid detection of surface anisotropy ($\Delta R/R \neq 0$ means that $R_x \neq R_y$) [2]. Then the detected anisotropy of plasmons in array of Au clusters is investigated in detail with the method of reflection of light polarized along the x and y axes. Given the direction of elongation of Au clusters, Figure 1, it is assumed in formula (2) and further, that $y \parallel [110]$ and $x \parallel [1\bar{1}0]$ for the indices α of light polarization. Independently measured reflectance anisotropy spectra $\Delta R/R$ and polarized reflection spectra R_α for Au/p-GaAs structure (Figure 1) are presented in Figure 3, *a* and *b*, respectively. All the spectra were obtained after annealing the sample at temperature of 350°C during 30 min. In spectrum $\Delta R/R$ in Figure 3, *a*, a negative feature is observed in the infrared range 0.4–1.3 eV, i.e. at much lower energies than are typical of Au nanoclusters of other types formed on GaAs(001) surface [2,3]. The negative sign and relatively low energy corresponding to the minimum of $\Delta R/R$ allows to attribute this feature to dipole plasmons whose polarization is in [110] direction of Au cluster elongation. In the same spectrum $\Delta R/R$, Figure 3, *a*, there is a positive feature in the range 1.3–2.2 eV which is associated with Au clusters plasmons polarized in $[1\bar{1}0]$ direction.

Spectra *1* and *2* in Figure 3, *b* express the reflection coefficients R_α for light polarized in $y \parallel [110]$ and $x \parallel [1\bar{1}0]$ directions, respectively. In Figure 3, *b*, spectrum *1* for light polarization $E \parallel [110]$ has a maximum at photon energy ~ 1 eV, the same as the energy of a minimum of spectrum $\Delta R/R$ in Figure 3, *a*. Similarly, a broad feature

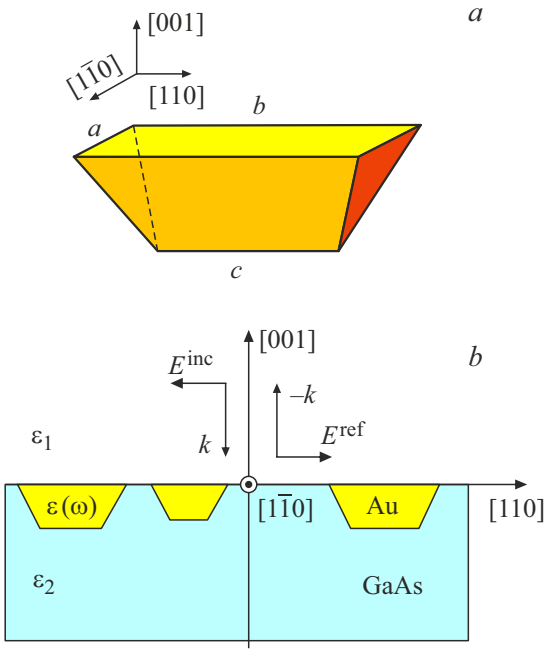

Figure 2. *a* — the wedge shape of a single cluster. *b* — a scheme of normal reflection of linearly polarized light from GaAs(001) surface with an array of wedge-shaped Au nanoclusters elongated in [110] direction.

in spectrum *2* for polarization $E \parallel [1\bar{1}0]$ is located in the range 1.3–2.2 eV just as a maximum in Figure 3, *a* which is characteristic of localized plasmons polarized orthogonally to the direction of elongation of Au clusters. The spectral features in Figure 3 observed for an array of clusters are considered to be inhomogeneously broadened since plasmons of the same polarization have different frequencies in clusters of different lengths (this property of the spectra is discussed further). It should be noted that an increase of film thickness for Au films with initial thicknesses 5–20 nm leads to a slight red shift of the peak with $\alpha = y \parallel [110]$ and a slight blue shift of the peak with $\alpha = x \parallel [1\bar{1}0]$. This means that the mean length of wedge-shaped Au (Au_2Ga) clusters formed in the same annealing regime turns out to be slightly longer for structures with thicker initial films.

3.2. Interpretation

Observed optical spectra are interpreted within the theory of polarized light reflection at normal incidence as sketched in Figure 2, *b*. The presence of a layer of elongated plasmon nanoclusters at the surface of semiconductor is taken into account. Dielectric permittivity of Au cluster material in actual range of frequency ω is approximated by expression

$$\varepsilon(\omega) = \varepsilon_\infty - \frac{\omega_p^2}{\omega^2 + i\omega\gamma(\omega)}. \qquad (3)$$

The plasma frequency ω_p, the inverse electron relaxation time $\gamma(\omega)$ and the background dielectric permittivity ε_∞

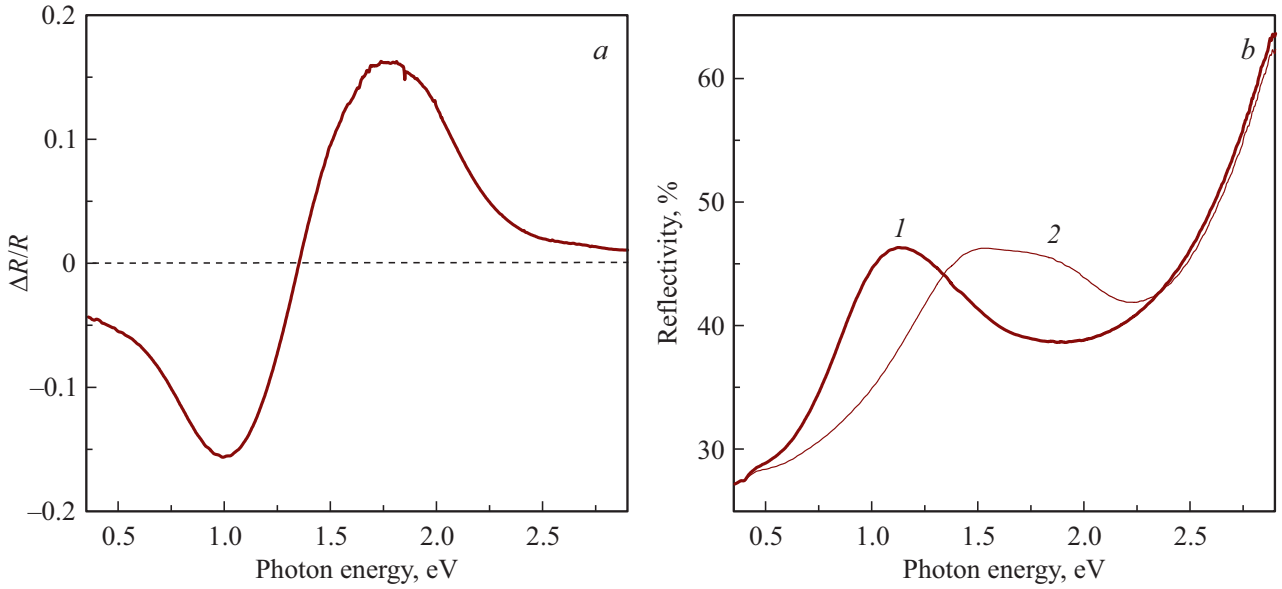

Figure 3. *a* — reflectance anisotropy spectrum $\Delta R/R$ and *b* — normal reflection coefficients of polarized light R_α with $\alpha = y \parallel [110]$ (*1*) and $\alpha = x \parallel [1\bar{1}0]$ (*2*), measured independently after annealing Au/*p*-GaAs structure at temperature 350°C film during 30 min. The thickness of initially deposited gold film is 5 nm.

are fitted to spectroscopy data for gold [8]. In plasma of a nanocluster with subwavelength sizes $\bar{a} \ll c/\omega$, the electric field $\mathbf{E}$ induces the dipole moment $\mathbf{p} = \hat{\chi}(\omega)\mathbf{E}$, where $\hat{\chi} = \hat{\chi}' + i\hat{\chi}''$ is the tensor of plasmon polarizability. In the principal axes, the tensor $\hat{\chi}$ of second rank is diagonal with components $\chi^{(\alpha)}(\omega - \omega_{\alpha,n})$ depending on exciting frequency, where $\omega_{\alpha,n}$ is the frequency of plasmon polarized along α-th axis in the cluster with number n.

Reflection coefficients of polarized light incident normally onto a two-dimensional array of identically oriented dipole plasmons with polarizabilities $\chi^{(\alpha)}(\omega - \omega_{\alpha,n})$ were calculated as described in [9]. Taking into account the field $\mathbf{E}(0)$ acting in the dipole layer, we obtain for the components of light field radiated along the normal with polarizations $\alpha = x$ or y the following equation

$$E_\alpha(z) = E_\alpha^{(0)}(z) + g_{\alpha\alpha}^{(0)}(z, \tilde{h})\,\frac{1}{L^2}\sum_n \chi^{(\alpha)}(\omega - \omega_{\alpha,n})E_\alpha^{(0)}(\tilde{h}). \tag{4}$$

Here, $g_{\alpha\alpha}^{(0)}(z, \tilde{h})$ is the Green's function and $E_\alpha^{(0)}(z)$ is the electric field with $\alpha = x$ or y in a layered medium without clusters, $1/L^2$ is the characteristic density of clusters in layer, and $\tilde{h} \ll c/\omega$ is the distance from the cluster layer to the crystal surface. Direct dipole-dipole interactions are neglected in (4) because the sizes of clusters are small ($ab \ll L^2$ in Figure 2), and the image effect of α-polarized dipole plasmon of n-th cluster is included formally in its frequency $\omega_{\alpha,n}$. Given the field functions [9], we obtain from (4) the expression $r_\alpha = r^{(0)} + \Delta r_\alpha$ for the amplitude coefficient of normal reflection of α-polarized light. It includes the coefficient $r^{(0)}$ of light reflection from isotropic surface vacuum/crystal without nanoclusters and the anisotropic plasmonic contribution

$$\Delta r_\alpha \sim \sum_n \chi^{(\alpha)}(\omega - \omega_{\alpha,n})$$

of clusters numbered by n. Our final goal is calculating the observable optical quantities: the normal reflection coefficient $R_\alpha(\omega) = |r_\alpha|^2$ of α-polarized light and the anisotropy signal (2).

Next, it is necessary to focus on the features of plasmonic polarizability tensor $\hat{\chi}$ of a wedge depicted in Figure 2, *a*. A numerical calculation of frequency-dependent $\hat{\chi}$ for a wedge, just as for other irregular polyhedra [10], would be very cumbersome, but its results would be of rather limited interest. Instead, here we discuss the problem qualitatively, using group-theoretic considerations. The point symmetry group of a wedge C_{2v} has the only axis of second order C_2, which defines one $C_2 \parallel z$ of the three orthogonal principal axes of tensor $\hat{\chi}$. The other two principal axes lying in the symmetry planes (110) and $(1\bar{1}0)$ are directed along the sides b and a of the base of wedge. Diagonal components $\chi^{(\alpha)}$ of the polarizability tensor are different in these principal axes. These properties are characteristic of the principal axes and polarizability components of an ellipsoid (point group D_{2h}). Therefore, in what follows we use the well-known expressions [10] for the polarizability of an ellipsoid or even a spheroid to interpret approximately the spectral and polarization properties of plasmons in a wedge. Inhomogeneity of environmental medium for a wedge is modeled using the effective permittivities varied in the interval $\varepsilon_1 < \varepsilon^{(\alpha)} < \varepsilon_2$ along the α axes.

For the described model, the polarizability components are reduced to the expression:

$$\chi^{(\alpha)}(\omega-\omega_{\alpha,n})=\frac{B^{(\alpha)}\omega_{\alpha,n}^2}{\omega_{\alpha,n}^2-\omega^2-i\omega\gamma_\alpha}, \qquad (5)$$

where $\omega_{\alpha,n}$ is the frequency of plasmon polarized along the α-th axis in the cluster with number n, $\gamma_\alpha=\gamma(\omega_{\alpha,n})$ with $\gamma_\alpha \ll \omega_\alpha$, and $B^{(\alpha)}$ takes account of the „background" polarizability of cluster and the transformation of light on the crystal surface in its reflection [9].

Given representation (5), we obtain estimates of inhomogeneously broadened spectra of light reflected from an array of nanoclusters with relative sizes $b/a>1$. The sum over cluster numbers n in (4) with plasmon polarizabilities (5) expresses, in essence, averaging over the plasmon frequencies $\omega_{\alpha,n}$ which are considered further as random variables ξ for each polarization α. For plasmon frequencies, we postulate a distribution function $w^{(\alpha)}(\xi-\bar{\omega}_\alpha)$ with normalization $\int d\xi w^{(\alpha)}(\xi-\bar{\omega}_\alpha)=1$, with a mean value $\bar{\omega}_\alpha$ and a width δ_α. In averaging the correction Δr_α caused by plasmons we use the following rule:

$$\sum_n \chi^{(\alpha)}(\omega-\omega_{\alpha,n}) \rightrightarrows \bar{B}^{(\alpha)}\omega^2\int d\xi\,\frac{w^{(\alpha)}(\xi-\bar{\omega}_\alpha)}{(\omega-\xi)^2+(\gamma_\alpha/2)^2}. \qquad (6)$$

Characteristic value $\bar{B}^{(\alpha)}\sim 1$ of coefficient $B^{(\alpha)}$ and $\gamma_\alpha=\gamma(\bar{\omega}_\alpha)$ are slightly dependent on frequency near $\bar{\omega}_\alpha$.

Estimates of inhomogeneously broadened spectra with functions $w^{(\alpha)}(\xi-\bar{\omega}_\alpha)$ corresponding to the Gauss and Cauchy distributions and even to the uniform distribution in an interval reveal a two-peak structure explaining mainly the shape of the observed spectra (Figure 3). This is illustrated next by the result of analytical calculation with the Cauchy distribution

$$w_\alpha(\xi-\bar{\omega}_\alpha)=(1/\pi)(\delta_\alpha/2)/[(\xi-\bar{\omega}_\alpha)^2+\delta_\alpha^2/4].$$

Using (6), we average the spectra $R_\alpha\approx|r^{0)}|^2+2\,\mathrm{Re}(r^{(0)}\Delta r_\alpha^*)$ and $\Delta R/R$, linearized in Δr_α at $|\Delta r_\alpha|\ll|r^{(0)}|$. As a result, we obtain the following expressions for inhomogeneously broadened polarized reflection spectra

$$R_\alpha(\omega)\approx R_0(\omega)+A_\alpha^{(+)}\frac{\omega(\Delta_\alpha/2)}{(\omega-\bar{\omega}_\alpha)^2+(\Delta_\alpha/2)^2} \qquad (7)$$

with $\alpha=x,y$ and reflectance anisotropy spectrum

$$\frac{\Delta R}{R}(\omega)=A_x^{(-)}\frac{\omega(\Delta_x/2)}{(\omega-\bar{\omega}_x)^2+(\Delta_x/2)^2} - A_y^{(-)}\frac{\omega(\Delta_y/2)}{(\omega-\bar{\omega}_y)^2+(\Delta_y/2)^2}. \qquad (8)$$

In formula (7) $R_0(\omega)=|r^{(0)}|^2$ is the coefficient of normal reflection of light by GaAs crystal surface without clusters. The width $\Delta_\alpha=\gamma_\alpha+\delta_\alpha$ of α-polarized plasmon peak in (7) and (8) consists of the constants of homogeneous γ_α and inhomogeneous δ_α broadening of the plasmon spectrum. The coefficients in expressions (7) and (8) have the structure $A_\alpha^{(\pm)}=(k_0V/L^2)|r^{(0)}|^{\pm1}F_\alpha$, where $k_0=\omega/c$, V stands for the cluster volume, and $F_\alpha\sim 1$ is associated with $B^{(\alpha)}$ from (6).

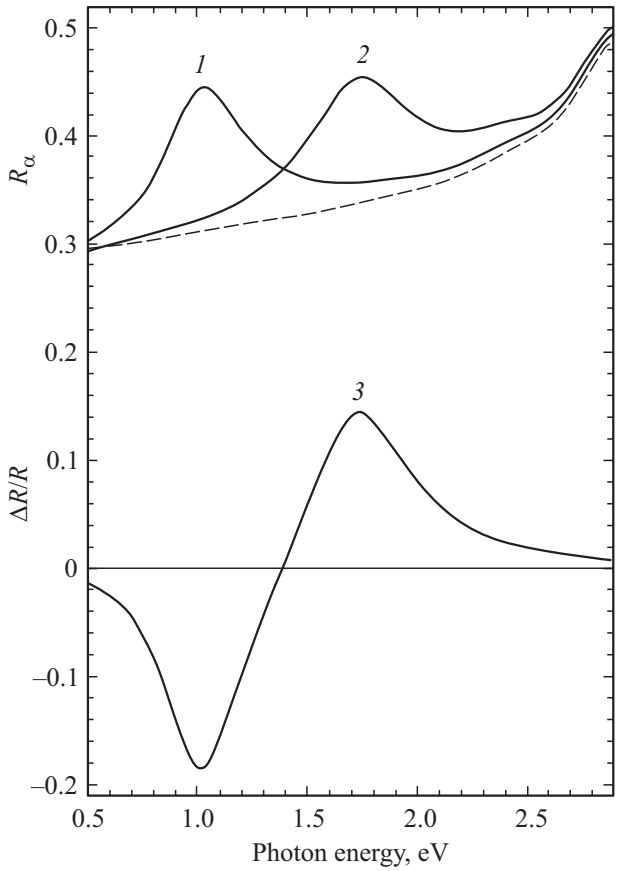

Figure 4. Results of simulation of inhomogeneously broadened spectra of polarized reflection R_y (*1*), R_x (*2*) and reflectance anisotropy spectrum $\Delta R/R$ (*3*) from the surface GaAs with a random array of elongated nanoclusters Au. The dashed line shows the spectrum R_0 of reflection from the GaAs surface without clusters.

Theoretical spectra (7) and (8), presented in Figure 4 agree with the experimental spectra seen in Figure 3. The theoretical spectra are calculated with the following parameters (eV): $\hbar\bar{\omega}_y=1$, $\hbar\bar{\omega}_x=1.7$, $\hbar\gamma_y=0.05$, $\hbar\gamma_x=0.1$, $\hbar\delta_y=0.4$, $\hbar\delta_x=0.5$. These estimates are made in the framework of the above model separately for each polarization of plasmons with taking account of the experimental data concerning the size of Au clusters (Figure 1). For quantitative agreement of the theory with the optical experiment (Figure 3 and 4), it is necessary to postulate the ratio $k_0V/L^2\sim 10^{-2}$, which is obtained with the experimental sizes a, b and h of nanoclusters, if $1/L^2\sim(10^{-1}-10^{-2})/ab$ and $\hbar\omega=1.5$ eV.

Thus, it is found that the wedge-shaped Au nanoclusters in Au/*p*-GaAs structures are elongated in [110]

direction on GaAs(001) surface. To compare, we note that on GaAs(001) surfaces passivated by monolayers of nitrogen or sulfur atoms before depositing of gold, the chains of Au nanoclusters elongated in $[1\bar{1}0]$ direction are formed [3]. In the two cases, difference in elongation directions of Au nanoclusters is explained by distinction of mechanisms of their formation. So elongation of Au clusters on passivated GaAs surfaces is due to the maximum rate of surface diffusion of gold atoms in $[1\bar{1}0]$ direction. In turn, elongation of wedge-shaped Au clusters studied in this work is related with the maximum rate of reaction (1) in [110] direction of nanoclusters growth.

4. Conclusion

This paper has presented the results of study of wedge-shaped gold (Au_2Ga) nanoclusters created on weakly oxidized *p*-GaAs(001) surface under high-temperature annealing of deposited Au film. The wedge shape and orientation of Au clusters are crystallographically determined: the rate of interaction between gold and gallium participating in cluster growth is large in [110] direction. A model is proposed of wedge-shaped cluster with a rectangular base on GaAs(001) surface and atomic faces coinciding with some planes of {111} family in GaAs crystal. Using optical spectra of normal light reflection from Au/*p*-GaAs(001) structures, the presence of strong anisotropy of resonant and polarization properties of plasmons localized on wedge-shaped Au nanoclusters was established. Polarization optical spectra are explained taking account of their inhomogeneous broadening associated with random relative length of clusters elongated in [110] direction. For wedge-shaped Au nanoclusters, it was found that the energies of plasmons with longitudinal [110] polarization occur in the near infrared region, and the energies of plasmons with $[1\bar{1}0]$ polarization are in the visible range.

Acknowledgments

The electron microscopic study was performed with the equipment of the Federal Common Use Centre „Materials Science and Diagnostics in advanced technologies“, supported by the Ministry of Education and Science of Russia.

Conflict of interest

The authors declare that they have no conflict of interest.

References

[1] A.A. Toropov, T.V. Shubina. *Plasmonic Effects in Metal-Semiconductor Nanostructures* (Oxford University Press, 2015).
[2] V.L. Berkovits, V.A. Kosobukin, V.P. Ulin, P.A. Alekseev, F.Yu. Soldatenkov, V.S. Levitskii. Phys. Status Solidi B, **259**, 2100394 (2022). https://doi.org/10.1002/pssb.202100394
[3] V.L. Berkowitz, V.A. Kosobukin, V.P. Ulin, P.A. Alekseev, F.Yu. Soldatenkov, V.A. Levitsky. FTP, **56**, 613 (2022). (in Russian). DOI: 10.21883/FTP.2022.07.52746.01
[4] A. Janas, B.R. Jany, K. Szajna, A. Kryshtal, G. Cempura, A. Kruk, F. Krok. Appl. Surf. Sci., **492**, 703 (2019). https://doi.org/10.1016/j.apsusc.2019.06.204
[5] D. Yan, E. Look, X. Yin, F.H. Pollak, J.M. Woodall. Appl. Phys. Lett., **65**, 186 (1994). https://doi.org/10.1063/1.113035
[6] A.J. Barcz, E. Kaminska, A. Piotrowska. Thin Sol. Films, **149**, 251 (1987). https://doi.org/10.1016/0040-6090(87)90301-4
[7] T. Yoshiie, C.L. Bayer, A.G. Milnes. Thin Sol. Films, **111**, 149 (1984). https://doi.org/10.1016/0040-6090(84)90483-8
[8] P.B. Johnson, R.W. Christy. Phys. Rev. B, **6**, 4370 (1972). DOI: 10.1103/PhysRevB.6.4370
[9] V.A. Kosobukin, A.V. Korotchenkov. FTT **58**, 2446 (2016). (in Russian). DOI: 10.21883/ftt.2016.12.43871.164
[10] V.V. Klimov. *Nanoplazmonika* (M., Fizmatlit, 2010). (in Russian).